Available online at www.sciencedirect.com
SCIENCE DIRECT®
Catalysis Today 87 (2003) 247–253
CATALYSIS TODAY
www.elsevier.com/locate/cattod

Hydrogen production by oxidative methanol reforming on Pd/ZnO catalyst: effects of Pd loading

Shetian Liu*, Katsumi Takahashi, Muneo Ayabe

Department of Industrial Machine & Plant Ind. Co Ltd., Environmental Process Development Center, Technical Research Laboratory, Ishikawajima-Harima Heavy Industries Co., Ltd., No. 1 Shin-Nakahara-Cho Isogo-ku Yokohama 235-8501, Japan

Abstract

Catalytic performances of Pd/ZnO in oxidative methanol reforming reaction were studied as a function of Pd loading. It was confirmed that the formation of Pd–Zn alloy is essential to the selective production of hydrogen. High active Pd/ZnO, comparable to commercial Cu-Zn catalyst, was obtained with higher Pd loading. Selectivity of the reaction was greatly increased by increasing Pd loading on ZnO. At higher Pd loadings (>5%), co-precipitation was superior to impregnation for the catalyst preparation. The catalytic performances were also discussed based on results from X-ray diffraction (XRD) characterization.

Keywords: Hydrogen production; Oxidative steam reforming; Methanol; Palladium; Zinc Oxide

1. Introduction

The use of hydrogen-fueled proton-exchange membrane fuel cells (PEMFCs) offers the potential of reducing carbon dioxide and nitric oxides emissions from vehicles. However, current technologies for on-board storage of hydrogen gas are still not economically attractive [1]. Among various on-board processing of liquid fuels oxidative methanol reforming (OMR) is regarded as the most promising method of supplying hydrogen to PEMFCs mounted in a vehicle [2–4].

The OMR reaction is a combination of partial oxidation (POM, Eq. (1)) with steam reforming (SRM, Eq. (2)) at such a ratio that the overall reaction is thermal-neutral or modestly exothermic. In reality, the OMR reaction can not be completely heat balanced ($\Delta H^\circ = 0$) because of heat loss. An almost heat balanced OMR reaction is illustrated in Eq. (3).

$$CH_3OH(1) + \tfrac{1}{2}O_2 \rightarrow CO_2 + 2H_2 \quad (\Delta H^\circ = -154.8\,\text{kJ/mol}) \tag{1}$$

$$CH_3OH(1) + H_2O(1) \rightarrow CO_2 + 3H_2 \quad (\Delta H^\circ = +131\,\text{kJ/mol}) \tag{2}$$

$$CH_3OH(1) + \tfrac{1}{2}H_2O(1) + \tfrac{1}{4}O_2 \rightarrow CO_2 + \tfrac{5}{2}H_2 \quad (\Delta H^\circ = -12\,\text{kJ/mol}) \tag{3}$$

Early studies on OMR reaction were reported by Huang and Wang [5,6]. They studied the effect of O_2 addition to SRM reaction and the kinetics of OMR reaction over Cu-Zn-Al catalysts. Recent studies by Velu et al. [7,8] and Murcia-Mascarós et al. [9] on Cu-Zn based catalysts revealed the high activity for methanol conversion and high selectivity for hydrogen production. However, the rapid deactivation of Cu-Zn based catalysts by sintering of the metal at temperature

* Corresponding author. Tel.: +81-45-759-2819; fax: +81-45-759-2206.
E-mail address: shetian_lyu@ihi.co.jp (S. Liu).

0920-5861/$ – see front matter © 2003 Elsevier B.V. All rights reserved.
doi:10.1016/j.cattod.2003.09.004

above e.g., 300 °C, obstructs its application in OMR process for on-board hydrogen production.

Pd/ZnO catalyst, initially studied by Takezawa and Iwasa [10], Takezawa and co-workers [11,12] for SRM reaction and by Cubeiro and Fierro [13,14] for POM reaction, demonstrated high activity and selectivity in both the SRM and POM reactions. The high selectivity of Pd/ZnO towards hydrogen production was proposed to relate to the formation of Pd–Zn alloy on the catalyst. Similar result on SRM reaction was also obtained recently by Chin et al. [15]. Considering the higher melting point of Pd compared with Cu, better thermal stability is expected for Pd/ZnO at higher reaction temperature. It thus promotes us to investigate its catalytic performances in OMR reaction.

2. Experimental

2.1. Catalyst preparation

The Pd/ZnO catalysts were prepared by either impregnation (IMP series) of a ZnO support (Sakai Co.) with $Pd(NO_3)_2$ aqueous solution (10% $Pd(NO_3)_2$ in 10% HNO_3 from Aldrich) or by co-precipitation (CP series) of $Zn(NO_3)_2$ + $Pd(NO_3)_2$ with NaOH + Na_2CO_3 aqueous solutions at constant pH and room temperature. $Zn(NO_3)_2{\cdot}6H_2O$, NaOH, and Na_2CO_3 of analytical grade were from wako chemicals. Pd weight loading for IMP samples was 1–10%, and the nominal Pd loading of CP samples was 1–15%. The catalysts were named according to their preparation method and nominal Pd loading. For example, the sample prepared by IMP method with 3.5% Pd was designated as IMP3.5, and the sample prepared by CP method with 15% Pd was designated as CP15, and so on. All the samples were finally calcined at 450 °C for 2 h and crushed to 0.15–0.25 mm for activity test.

2.2. Catalytic reaction

The catalytic reactions were carried out in a conventional flow fixed-bed quartz reactor of 6 mm i.d. using 0.3 g of catalyst at atmospheric pressure. Prior to the reaction, the catalyst was reduced in situ in a stream of 20% H_2 in N_2 (160 ml/min) at 400 °C for 2 h. After cooling down to the reaction temperature (250 °C), methanol+water mixture (H_2O/CH_3OH molar ratio = 1.5) was fed into a vaporizer by a mini–micro liquid pump at a rate of 0.44 g/min and conveyed into the reactor by N_2 as both carrier gas and internal standard for product analysis. The N_2 flow was adjusted precisely by a STEC mass flow controller at a rate of 120 ml/min. O_2 adjusted by another mass flow controller was fed into the reactor at a rate of 16.7 ml/min, which gave an O_2/CH_3OH ratio of 0.1. The above conditions determined a gas hourly space velocity (GHSV) of ∼110,000 h^{-1}. After reaction, the product gases were passed through a cold-water (5 °C)-circulated condenser followed by a water-scrubber kept in ice water. The scrubbed gases were analyzed on-line using a Shimadzu GC-8A gas chromatograph automatic analysis system equipped with Parapak-Q and molecular sieve 13X columns. Unless otherwise mentioned, the initial activity was evaluated from the data collected between 1 and 3 h of reaction time on stream. The gas yield (moles of CO_2 + CO produced per mole of methanol fed) was used as a measure to compare catalyst activity. Selectivity of the reaction was defined as moles of CO_2 produced per mole of CO_2 + CO in the products.

For comparison, a commercial Cu-Zn based catalyst (MDC-4) from Süd–Chemie was also evaluated under the same reaction conditions.

2.3. Catalyst characterization

Powder X-ray diffraction (XRD) patterns of the samples were recorded on a Rigaku RINT1100 diffractometer with a Cu Kα (λ = 0.15406 nm) radiation. Scanning 2θ angles were ranged from 10 to 80°. The Scherrer equation ($D_{hkl} = K\lambda/\beta\cos\theta$, $K = 0.94$) was applied to the diffraction peaks of ZnO(1 0 1) and Pd–Zn(1 1 1) to calculate the corresponding crystal size based on the line broadening. However, the results are used only for relative comparison of the mean crystal size.

3. Results and discussion

3.1. X-ray diffraction

Fig. 1a shows the XRD patterns of the calcined IMP samples. With IMP1, only diffractions from ZnO could be observed. The diffraction line attributed to PdO at

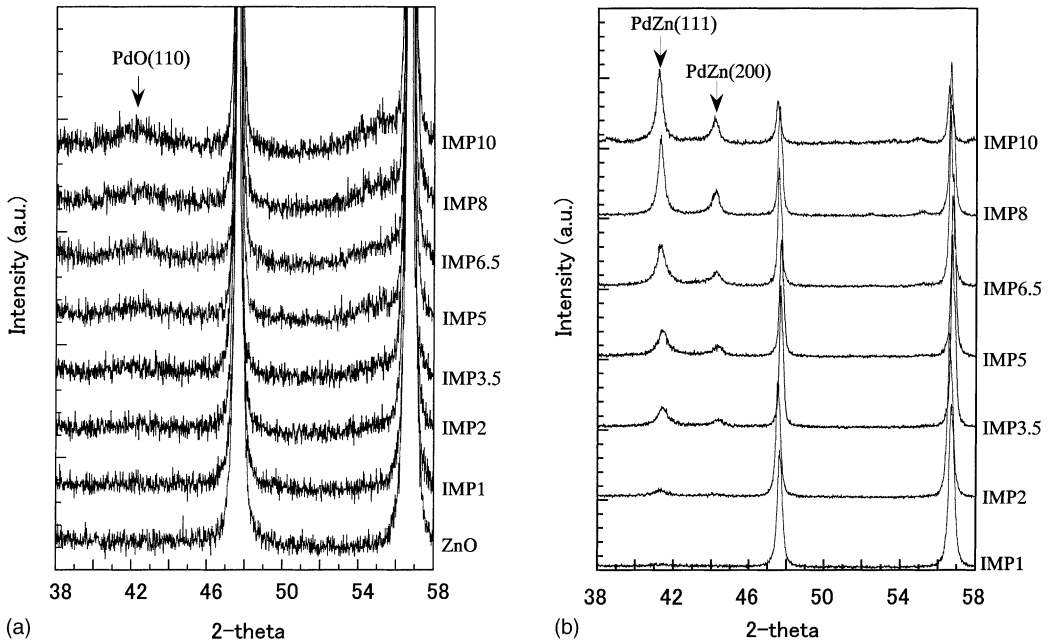

Fig. 1. Powder XRD patterns of freshly prepared (a) and spent (b) IMP catalysts.

2θ of 42.1° was appeared at Pd loadings exceeding 2%. Though broad and weak, the PdO diffraction line became stronger with the increase of Pd loading. Variation in intensities of ZnO diffraction lines was also noticed. After activity test, XRD patterns (Fig. 1b) of spent IMP samples indicated new diffraction lines at 2θ of 41.2 and 44.2°, and their intensities increased with the increase of Pd loading. Considering that the diffractions from Pd and Zn metals should appear at 40.1° for Pd(1 1 1) and 43.3° for Zn(l 0 1), they were indexed to the diffractions of Pd–Zn(1 1 1) and Pd–Zn(2 0 0), respectively. This result is consistent with that reported by Iwasa et al. [11] and Cubeiro and Fierro [13]. It is believed that the Pd–Zn alloy was formed during the pre-reduction before OMR reaction.

Fig. 2 shows variation in XRD mean crystal size determined from line broadening of ZnO(1 0 1) and Pd–Zn(1 1 1) diffraction. ZnO crystallites of fresh catalysts increased in size with the increase of Pd loading and at Pd loading above 5% became essentially constant. After activity test the size of ZnO crystallites were unexpectedly noted to decrease to and remain the same as that of original ZnO support. The $Pd(NO_3)_2$ solution for catalyst preparation contained 10% HNO_3 and consequently the ZnO support was partially dissolved during impregnation. After drying and calcinating, larger ZnO crystallites could be developed on the catalyst surface. For higher Pd loadings, more ZnO was dissolved in solution, and thus increased the size of newly formed ZnO crystallites. On

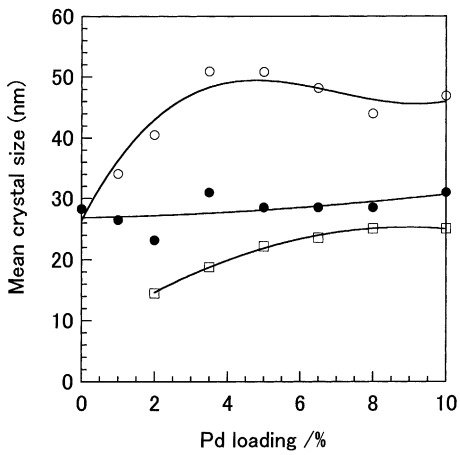

Fig. 2. Mean size of ZnO ((○) freshly prepared; (●) spent) and Pd–Zn ((□) spent) crystallites of IMP catalysts.

the other hand, the presence of Pd(II) ions may also enhance the crystallinity of surface ZnO crystallites, and the heterogeneity of ZnO surface was increased by such kind of surface reconstruction. However, the new ZnO crystallites should be tightly connected to PdO particles. During the reduction in 20% H_2 gas flow at 400 °C, the ZnO crystallites reacted with PdO to form Pd–Zn alloy. The ZnO support, not affected during impregnation, remained essentially unchanged subsequent to the reduction and OMR reaction. This is reasonable in consideration of the drastic reduction in the mean crystal size of ZnO crystallites for fresh samples compared to those spent samples, as evident from Fig. 2. Variation of the size of Pd–Zn crystallites as determined from Pa–Zn(1 1 1) line broadening is also indicated in Fig. 2. The size of Pd–Zn alloy crystallites increased with the increase of Pd loading, suggesting poor dispersion of the Pd–Zn alloy at higher Pd loadings.

XRD patterns for fresh CP samples are shown in Fig. 3a. At Pd loading below 15%, the patterns were very similar to that of IMP samples. However, the intensity of ZnO diffraction lines was lower than the IMP samples. The PdO diffraction peak at 2θ of 42.1° appeared at Pd loading above 3.5%, and the line intensity increased with Pd loading. The diffraction peaks for the Pd–Zn alloy at 2θ of 41.2 and 44.2° of spend CP samples (Fig. 3b) were quite different from that of spent IMP samples, being much broaden, suggesting more amorphous or smaller Pd–Zn crystallite formation for the CP samples.

The variation of ZnO and Pd–Zn alloy crystal size with Pd loading is indicated in Fig. 4. In contrast to IMP samples, the fresh CP samples showed similar ZnO crystal size from 12 to 18 nm. After the OMR reaction, ZnO crystal size of the spent CP samples kept at around 15 nm, which was smaller than the IMP samples (∼30 nm).

Comparing with IMP samples, the variation of Pd–Zn crystal size with Pd loading of spend CP samples was more complex. The Pd–Zn crystallites of samples with Pd loadings below 3.5% were expected to be small due to the low Pd content. For spent samples of CP5, CP6.5, and CP8, the mean crystal size of Pd–Zn alloy was 15–16 nm, much bigger than that of CP10 and CP15, which was estimated as 7–8 nm. It seems that a sudden decrease in the crystallinity of Pd–Zn alloy occurred with Pd loading above 10%. In

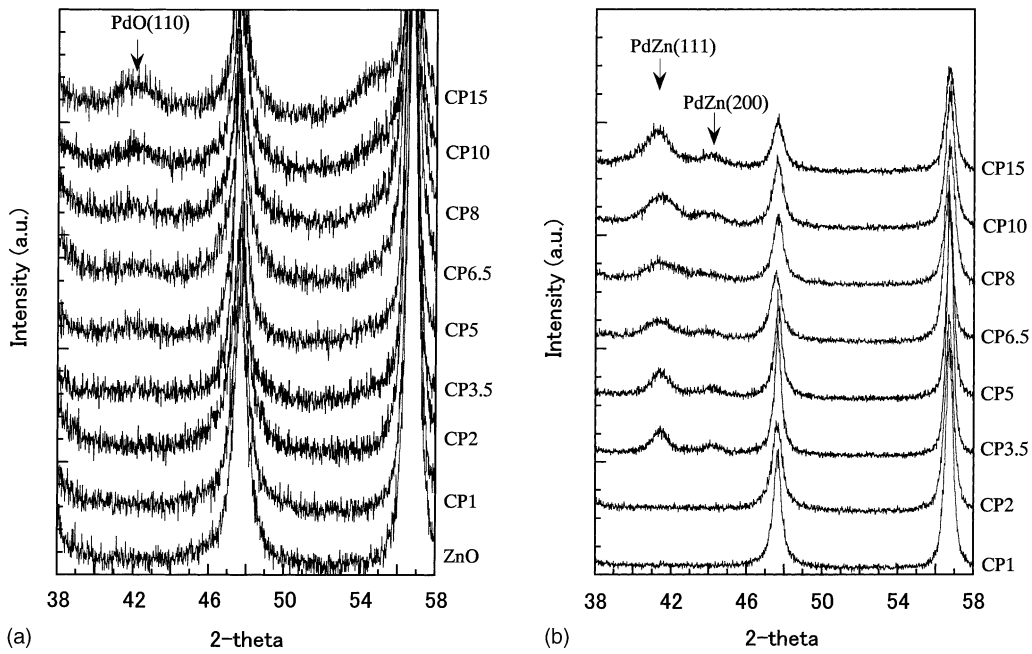

Fig. 3. Powder XRD patterns of freshly prepared (a) and spent (b) CP catalysts.

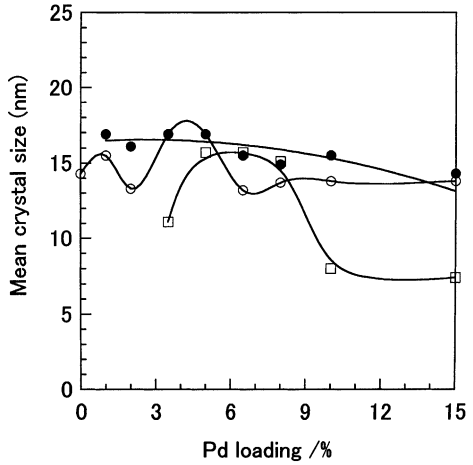

Fig. 4. Mean size of ZnO ((○) freshly prepared; (●) spent) and Pd–Zn ((□) spent) crystallites of CP catalysts.

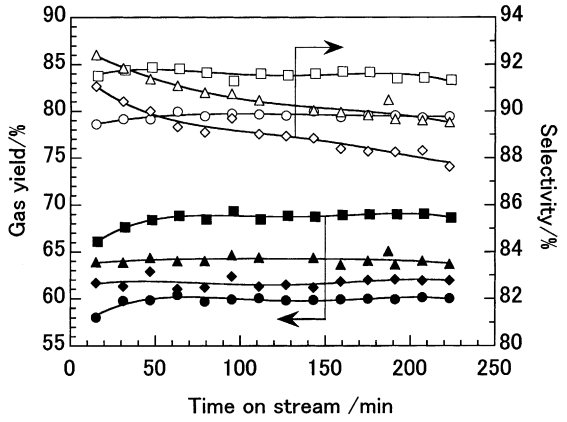

Fig. 5. Variation of gas yield (solid symbol) and selectivity (open symbol) with reaction time on stream for OMR reaction over CP3.5 (○),(●) CP6.5 (□), (■) IMP3.5 (◇), (◆) and IMP6.5 (△), (▲) catalysts.

addition, it needs to point out that the size of Pd–Zn crystallites was similar to that of ZnO support for the spent CP samples, and at Pd loadings above 5% the Pd–Zn crystallites was smaller than that of IMP samples. These results suggested that the CP samples were more homogeneous, and the dispersion of Pd–Zn alloy was higher than that for corresponding IMP samples.

3.2. Stability of Pd/ZnO catalysts

As stated in the introduction, Pd/ZnO is a good catalyst in SRM and POM reactions. It is also anticipated to perform well in OMR reaction. However, experimental data for application to OMR reaction are limited in literature for this catalyst. The present results confirmed its good applicability, and excellent performances were achieved with Pd/ZnO catalyst. The main products are hydrogen and carbon dioxide. Carbon monoxide production in minor amount depends on the catalyst. Being a poison to the electrocatalyst at the fuel cell anode, special attention was paid to decrease CO formation during the study.

Fig. 5 shows the variation of gas yield and selectivity with reaction time on stream of several IMP and CP samples. Within 4 h of reaction, no decrease in gas yield and selectivity was observed for the CP samples. All the CP samples appeared to be rather stable in OMR reaction under the examined conditions. Gas yield on CP6.5 was 68% at a selectivity of 92%. For IMP samples, gas yield was stable during 4 h reaction, but the selectivity decreased with reaction time on stream. XRD results indicated CP samples to be more homogeneous than IMP samples and this would appear to be the reason for their better stability in OMR reaction. The surface heterogeneity caused by dissolution of ZnO during impregnation of IMP samples may accelerate the change in Pd–Zn crystallites and Pd–Zn alloy composition during the oxidative reforming with consequent reduction in reaction selectivity and increased CO formation.

In Fig. 6 CP15 and the commercial Cu-Zn catalyst are compared and gas yield can clearly be seen to be more stable with CP15. At 4 h reaction, gas yield on CP15 was maintained at nearly 74% while with Cu-Zn, the initial 80% yield decreased to only 73%. The activity of CP15 was found comparable to the commercial Cu-Zn catalyst in OMR reaction, and the selectivity was lower than the Cu-Zn catalyst. CO (dry and N_2 free base) in product gases for the commercial Cu-Zn catalyst was 4200 ppm while on CP15 12000 ppm CO was produced. In consideration of the poisoning effect of CO to the PEMFCs anode, to increase the reaction selectivity and decrease CO formation is essential in developing an advanced Pd/ZnO catalyst for OMR reaction.

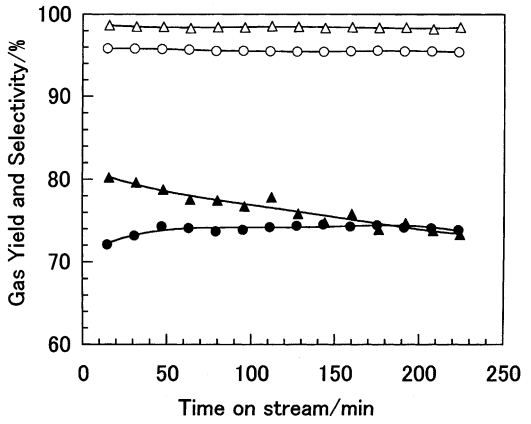

Fig. 6. Variation of gas yield (solid symbol) and selectivity (open symbol) with reaction time on stream for OMR reaction over CP15 (○), (●) and MDC-4 (△), (▲) catalysts.

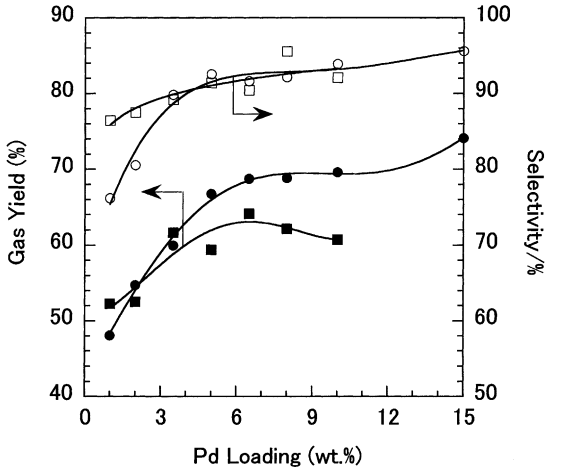

Fig. 7. Dependence of gas yield (solid symbol) and selectivity (open symbol) on Pd loading of CP (○), (●) and IMP (□), (■) catalysts for OMR reaction.

3.3. Effect of Pd loading

Pd–Zn alloy formation has been shown responsible for the high selectivity in SRM and POM reactions [11,13]. In the view of that OMR reaction is a combination of SRM with POM, catalytic performances of Pd/ZnO in OMR reaction is thus expected to closely relate to the particular state of Pd–Zn alloy on the ZnO support. XRD characterization indicated Pd–Zn crystallites of spent samples to strongly depend on Pd loading, which was also reflected in the catalytic performances of Pd/ZnO catalysts. The dependence of gas yield on Pd loading with IMP and CP samples is illustrated in Fig. 7. The gas yield was greatly increased at low Pd loading, but assumed essentially constant value at about 5%. The rapid increase in gas yield was considered due to greater surface concentration or surface area of Pd–Zn alloy. With increase in Pd loading, Pd–Zn crystallites grew larger, which inhibited further increase in the surface concentration of Pd–Zn alloy and resulted in a relative constant gas yield at 5–10% Pd loadings. Above 10%, gas yield for CP samples again increased though only moderately. The smaller Pd–Zn crystallites of these samples may have contributed to higher gas yield.

Fig. 7 also shows that, for Pd loading below 5%, IMP samples performance was better than that for CP samples, this being due to the greater surface concentration of Pd–Zn alloy for IMP samples. Nevertheless, at higher Pd loading, CP samples were more active than IMP samples. The highly active Pd/ZnO catalyst, essentially to the same extent as commercial Cu-Zn catalyst, can be produced at higher Pd loading.

Variation in selectivity as a function of Pd loading was actually the same as that noted for gas yield. The selectivity of CP samples sharply increased with rise in Pd loadings from low values. The selectivity on CP1 was 76% and more than 92% on CP5. CO formation is thus shown to greatly decrease with increase in Pd on ZnO. IMP selectivity exceeded that of CP samples at Pd loadings less than 5%. Larger Pd–Zn alloy crystallites or well crystallized Pd–Zn alloy particles would appear to have higher selectivity towards the OMR reaction. In the case of lower Pd loadings as with CP1 and CP2, Pd–Zn crystallites should be quite small and single Pd atoms may possibly be present in the catalyst. Such Pd atoms and/or very small non-perfect Pd–Zn alloy crystallites may possibly not be selective in the OMR reaction and promote CO formation.

At Pd loading above 5%, the selectivity of IMP and CP samples increased but slightly. On CP15 it was 95.5%, only 3% above that on CP5. The larger Pd–Zn alloy crystallite size may have been the reason for this, but with attainment of a certain size, any further increase would not likely have significant effect on the

selectivity of the catalyst. For reasons not presently explainable, further characterization of the catalyst surface may possibly provide some clarification.

4. Conclusion

Dependence of the catalytic performances of Pd/ZnO in OMR reaction on Pd loading was investigated using catalysts prepared by impregnation and co-precipitation. Both Pd/ZnO catalysts exhibited high activity and selectivity in OMR reaction for hydrogen production. Highly stable catalysts could be obtained by co-precipitation at higher Pd loading values. Pd–Zn alloy formation was confirmed by XRD characterization of freshly prepared and spent catalysts. Catalyst activity was strongly related to crystal size and dispersion of Pd–Zn alloy on the ZnO support. With increase in Pd on ZnO, catalyst activity and selectivity significantly increase and CO formation is effectively reduced.

References

[1] D.L. Trimm, Z.I. Önsan, Catal. Rev. 43 (1-2) (2001) 31.
[2] L.F. Brown, Int. J. Hydrogen Energy 26 (2001) 381.
[3] S. Ahmed, M. Krumpelt, Int. J. Hydrogen Energy 26 (2001) 291.
[4] J.E. Funk, Int. J. Hydrogen Energy 26 (2001) 185.
[5] T.J. Huang, S.W. Wang, Appl. Catal. 24 (1986) 287.
[6] T.J. Huang, S.W. Wang, Appl. Catal. 40 (1988) 43.
[7] S. VeIu, K. Suzuki, M. Okazaki, M.P. Kapoor, T. Osaki, F. Ohashi, J. Catal. 194 (2000) 373.
[8] S. Velu, K. Suzuki, M. Okazaki, M.P. Kapoor, F. Ohashi, T. Osaki, Appl. Catal. A 213 (2001) 47.
[9] S. Murcia-Mascarós, R.M. Navarro, L. Gómez-sainero, U. Costantino, M. Nocchetti, J.L.G. Fierro, J. Catal. 198 (2001) 338.
[10] N. Takezawa, N. Iwasa, Catal. Today 36 (1997) 45.
[11] N. Iwasa, S. Masuda, N. Ogawa, N. Takezawa, Appl. Catal. A 125 (1995) 145.
[12] N. Iwasa, O. Yamamoto, T. Akazawa, S. Ohyama, N. Takezawa, J. Chem. Soc., Chem. Commun. (1991) 1322.
[13] M.L. Cubeiro, J.L. G Fierro, J. Catal. 179 (1998) 150.
[14] M.L. Cubeiro, J.L.G. Fierro, Appl. Catal. A 168 (1998) 307.
[15] Y.H. Chin, R. Dagle, J. Hu, A.C. Dohnalkova, Y. Wang, Catal. Today 77 (2002) 79.